International Journal of Recent Technology and Engineering (IJRTE)
ISSN: 2277-3878, Volume-8 Issue-3, September 2019

An Efficient Optimized Probabilistic Neural Network Based Kidney Stone Detection and Segmentation over Ultrasound Images

Raju.P, Malleswara Rao.V, Prabhakara Rao.B

Abstract: ***Locating renal calculus in the ultrasound image is a demanding requirement in the field of medical imaging. For accurate detection of kidney stone, in this paper, optimal recurrent neural network (OPNN) is adopted. The proposed work undergoes pre-processing, feature extraction, classification, and segmentation. Initially, the noise present in input images is removed with the median filter because noises impact the accuracy of the classification. Then, compute features of this image. In the classification stage, features are used to classify defects through optimal probabilistic NeuralNetwork (OPNN). OPNN is a combination of PNN and spider monkey optimization (SMO). The parameter of PNN is optimized with the help of SMO. Then, the stone region from the abnormal image is segmented using probabilistic fuzzy c-means clustering (PFCM). The proposed methodology performance can be analyzed by using Sensitivity, Accuracy, and Specificity.***

Keywords: Kidney stone, optimal recurrent neural network, feature extraction, spider monkey optimization, probabilistic fuzzy c-means clustering.

I. INTRODUCTION

Recent information from a few nations recommends a world-wide increment in the predominance of stone sickness in the last 3 to 4 decades. An assortment of purposes behind expanded stone pervasiveness has been postulated, with the basic supposition that natural variables, instead of hereditary ones, are capable, on account of the moderately brief time course over which these epidemiologic patterns have been observed [1]. Renal calculus disease is world's problem where in any delay in the detection can lead to loss of a life [2].Ultrasonic (US) images are used for analyzing and locating renal diseases [3]. Different pattern recognition and noise removal methods are used to identify and locate diseases [4].

The identification of the kidney stone diseases in early stage is helpful for better treatment [5]. The process of formation of kidney stones is mentioned in [6]. Few types of the kidney stones appear quite commonly in human body [7].

Manuscript published on 30 September 2019
*Correspondence Author
Raju.P*, Research scholar, Dept of ECE, JNTU Kakinada, Andhra Pradesh, India.
MalleswaraRao.V, Professor, Dept of ECE, GITAM, Visakhapatnam, Andhra Pradesh, India.
PrabhakaraRao.B, Program Director, dept Nanotechnology, JNTU Kakinada, AndhraPradesh, India,

© The Authors. Published by Blue Eyes Intelligence Engineering and Sciences Publication (BEIESP). This is an open access article under the CC-BY-NC-ND license http://creativecommons.org/licenses/by-nc-nd/4.0/

Identification proof of stones in the urinary area giving different side effects has been an issue for clinicians from days of yore and there are many sources for acquiring medical images [8].

Ultrasound is significant for the clinician to decide the health of the kidneys and furthermore to envision any abnormalities present in the kidneys. US machines with programmed recognition in the present market were expanding these days. Yet, this expanding was greater part in other fields than the kidney, for example, to recognize little tumor in the bosom and to identify chromosome abnormalities in hatchling [9]. Kidney images with a stone are analyzed using computerized tomography is a standard technique in demonstrating a high affectability (96%–98%) and particularity (96%–100%) [10]. Renal calculus is most widely spreading disease which gradually harms the human life. Early recognition of stones helps to diagnose patients [11].

II.LITERATURE SURVEY

A Lot of researchers have developed ultrasound stone detection and classification. Wan MahaniHafizah*et al* [12], have presented a methodology of highlight extraction of renalUS images dependent on 5 intensity histogram highlights and 19 dim level co-event lattice (GLCM) highlights. Renal US images were partitioned into 4 unique gatherings; normal, cystic infection, bacterial contamination, and kidney stones. Before highlight extraction, the pictures were at first preprocessed for safeguarding pixels of enthusiasm preceding element extraction. Preprocessing procedures including the district of enthusiasm editing, form recognition, picture revolution, and foundation evacuation, have been connected. Test outcome demonstrates that kurtosis, Average, skewness, cluster shades, and cluster noticeable quality commands over different parameters.

Mariam WagihAttia*et al* [13] has presented an automatic arrangement of five different renal diseases were considered. A lot of measurable features were extricated from the region of interest.By using chosen features a neural system classifier is developed. A right order pace of 97% has been gotten utilizing the multi-scale wavelet-based features.

Koushal Kumar and Abhishek [14], have presented to analyze renal calculus sickness by utilizing 3 distinctive neural system methods that have diverse design and qualities. That work aimed to analyze the presentation of each of the three neural networks based on accuracy.For the diagnosing renal calculus disease, Learning vector quantization (LVQ), two layer feed-forward perceptron prepared with back proliferation preparing algorithm and Radial basis function (RBF) systems are utilized.

The informational index utilized for diagnosis was true information with 1000 occasions and 8 properties. They check the presentation correlation of various calculations for renal calculus diagnosis that help in early detection and less time.

AbhinavGupt and Sunanda Kaushal [15], have presented and analyze two completely programmed and unaided techniques for B-mode US images stone discovery. The main algorithm uses the upside of the Speckle reducing anisotropic diffusion strategy, and the subsequent depended on the log decompression model.

Gayathri Varmaet al [16], have presented to identify the urinary stone disease.200 patients having urinary stone illness for least a half years were interviewed. They were named demonstrated stone patients simply after recovery. The viability of the underlying screening investigation was evaluated to ascertain the explicitness and affectability of the two modalities of investigation.

M. R. Bailey et al [17], have presented the physical instrument in HIFU. Other mechanical impacts from ultrasound seem to invigorate a resistant reaction, and air pocket elements assume a significant role in lithotripsy and ultrasound-improved drug conveyance. In couple of years a sensational move to comprehend these nonlinear and mechanical components has happened. Explicit difficulties stay, for example, treatment convention arranging and constant treatment observing. These difficulties can be overcome by an upgraded comprehension of the physical mechanisms.

III. PROPOSED KIDNEY STONE DETECTION METHODOLOGY

Kidney stone detection and segmentation is a major process in the medical field. Early detection may easily cure diseases. So, in this paper, efficient kidney stone detection is proposed. The proposed system consists of four modules namely, preprocessing, feature extraction, classification, and segmentation. Initially, the images are preprocessed with the assistance of the middle channel. Then, GLCM features and First Order Statistical highlights are extracted from the preprocessed image. Based on the highlights the stone image is classified using the optimal probabilistic neural network (OPNN). To enhance the PNN, the parameter of the PNN classifier is optimized using SMO. Then, the abnormal region of the US image is separated using PFCM. The overall chart of the proposed procedure is given in fig.1.

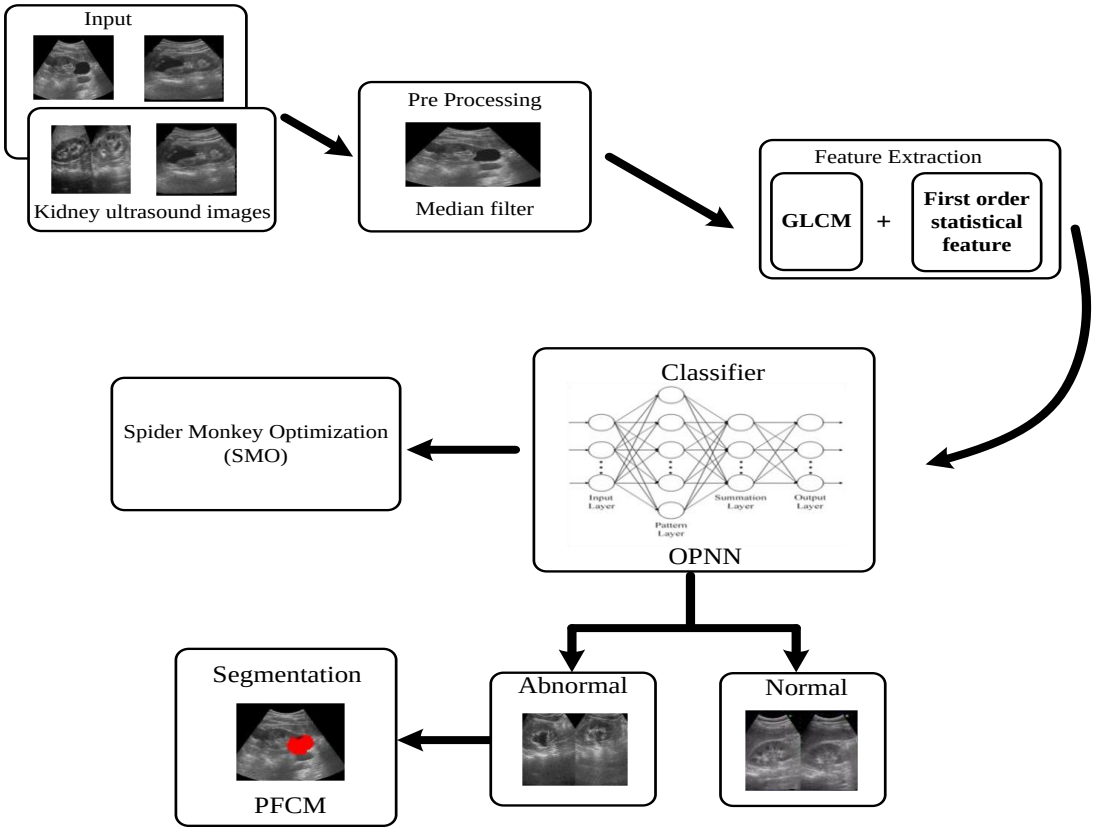

Fig.1. Proposed kidney stone detection and classification

A. Preprocessing

It is an important process of ultrasound images because these images are more prone to noise than other imaging methods. The ultrasound images are most part undermined by speckle noise. The noisy images cannot give higher classification and segmentation accuracy. A median filter is chosen for this purpose as it removes noise as well as holds the edges. This output de-noised image is used for further processing.

B. Feature extraction

Here, the GLCM features and First Order Statistical Features are separated from the de-noised image.

Totally, twenty-two features are available in GLCM. Among them five important features namely, Correlation, Contrast, Energy, Entropy and Sum of Squares. Similarly, in this paper, first order factual features also separated from the info image and are fed to the classifier. The extracted features are listed below.

C.GLCM features extraction

Correlation (F1): Correlation is the span that ponders the relationship between pixels and its region pixels. The relationship is characterized by the ensuing equation as,

$$Corr = \sum_{r=0}^{P-1}\sum_{s=0}^{P-1}\frac{[r*s]*\log(M(r,s))-[\mu_b*\mu_c]}{\sigma_b*\sigma_c} \quad (1)$$

Where μ_b, μ_c and σ_b^2, σ_c^2 are the mean and variance of r, s, are given as,

$$\mu_b=\sum_{r=0}^{P-1} r\sum_{s=0}^{P-1}M(r,s) \quad ; \quad \mu_c=\sum_{r=0}^{P-1} s\sum_{s=0}^{P-1}M(r,s) \quad (2)$$

$$\sigma_b^2=\sum_{r=0}^{P-1}\left(I_b(r)-\mu_b(r)\right)^2 \quad \sigma_c^2=\sum_{s=0}^{P-1}\left(I_c(s)-\mu_c(s)\right)^2 \quad ; \quad (3)$$

Contrast (F2): In perspective on the neighborhood homogeneity of an image, differentiation is characterized as the distinction in luminance. Besides, the contrast is characterized utilizing the resulting equation.

$$Cont=\sum_{p=0}^{P-1}p^2\left\{\sum_{r=1}^{P}\sum_{s=1}^{P}M(r,s)\right\}, |r-s|=p \quad (4)$$

Where, $M(r,s)$ is the Co-occurrence Matrix.

Energy (F3): Moreover, the energy likewise controls the image homogeneity. The energy can be connoted as pursues,

$$Ene=\sum_{r=0}^{P-1}\sum_{s=0}^{P-1}M(r,s)^2 \quad (5)$$

Entropy (F4): It measures the information of an image to empower picture pressure by estimating the loss of image information. The entropy can be verbalized as pursues.

$$Ent=-\sum_{r=0}^{P-1}\sum_{s=0}^{P-1}M(r,s)*\log(M(r,s)) \quad (6)$$

Variance (F5):

$$V=\sum_{r=0}^{P-1}\sum_{s=0}^{P-1}(r-\mu)^2\ M(r,s) \quad (7)$$

D. First order statistical features

Mean (F6): The average of the image is called as means. It can be written using equation (8).

$$\mu=\sum_{x=1}^{N_g}x.p(x) \quad (8)$$

Variance (F7): The intensity variation of the image is calculated using variance. It is given in equation (9)

$$\sigma^2=\sum_{x=1}^{N_g}(x-\mu)^2.p(x) \quad (9)$$

Skewness (F8): It describes the intensity of a darker or lighter colour. It is calculated using equation (10).

$$S_k=\sigma^{-3}\Sigma_{x=1}^{N}g_1(x-\mu)^3.p(x) \quad (10)$$

Kurtosis (F9): this feature gives homogeneity in intensity distribution. The Kurtosis is calculated using equation (11).

$$K_k=\sigma^{-4}\Sigma_{x=1}^{N}g_1(x-\mu)^4.p(x)-3 \quad (11)$$

Where, $p(x)$ is Ng/N with N as total number of pixels.

E. OPNN based classification

The removed features of input pictures are taken to be the input for our proposed classification algorithm. A novel PNN classifier is utilized to recognize the normal and abnormal type of image. PNN is quicker to train as compared to feed-forward backpropagation (FFBP) neural network. In any case, there is an exceptional issue related to PNNs that is optimizing its weight function which assumes a critical role, and is frequently information subordinate. In the present paper, a basic and powerful optimization method has been utilized to tackle this kind of numerical issue SMO optimization by which the network weight gets optimized. The PNN structure is shown in Fig. 2. The computation of OPNN based classification is explained below.

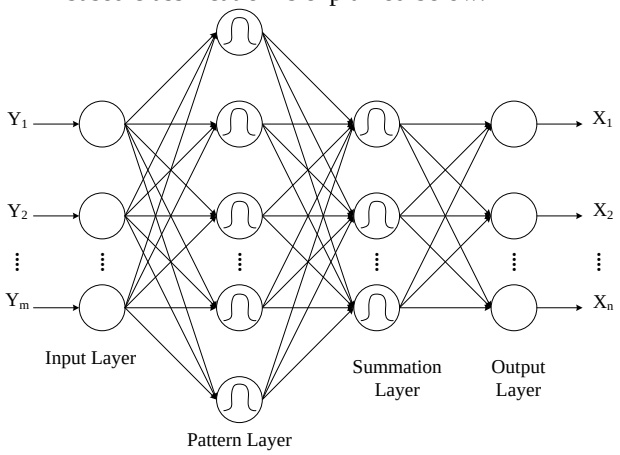

Fig.2. Structure of PNN

Step 1: The extracted features fed to PNN. Network starts estimation of the training test which is given by

$$Y=(y_1,y_2,\ldots y_m)^T \quad (12)$$

Step 2: Radial basis function demonstrates the likelihood of the trained data given by:

$$N_{ji}(Y)=\frac{1}{(2\pi\sigma^2)m/2}\exp\left(\frac{\|Y-W_{ji}\|}{2\sigma^2}\right) \quad (13)$$

Where σ determines ringer molded bend.

Step 3: Middle layer computes R given by

$$R_j(Y)=\sum_{j=1}^{M}w_{ji}N_{ji}(Y),\ j\in\{1,2,\ldots,m\} \quad (14)$$

Where w_{ji} denotes mixed weights and it subjects to

$$\sum_{j=1}^{M}w_{ji}=1,\ j\in\{1,2\ldots,m\}$$

Here $w_{ji} \in [0,1]$

Step 4: Output layer expressed as

$$O(Y) = \arg\max_{1 \le j \le m}(R_j) \quad (15)$$

Output of neuron which possesses the biggest likelihood thickness capacity is 1; the output of other neuron is 0·

Step 5: Error value can be calculated using equation (16).

$$Error = T\arg et - O(Y) \quad (16)$$

The error value should be minimum for classification process. To further reduce the value, the weight values are adjusted. The weight values are optimally selected with the help of spider monkey optimization (SMO).

Step 6: The random weight values are given to the input of the SMO algorithm. SMOA mimics food searching behavior of spider monkeys. This conduct can be grouped in four stages dependent on the idea of fission–fusion social structure (FFSS) of creepy crawly monkeys. To begin with, the gathering assesses the good ways from the food and afterward begins sustenance scavenging. In the subsequent advance, the places of gathering individuals and the assessed good ways from the sustenance sources is refreshed. In the following stage, the neighborhood chief updates its best position inside the gathering. All the gathering individuals begin looking through the sustenance on account of the absence of best position updation by the neighborhood head. In fourth step, the worldwide pioneer refreshes its ever best position. The gathering is splitted into littler subgroups on account of stagnation (no updation in worldwide pioneer position for a predefined time). The local leader limit (LLL) is connected to lessen the event of stagnation by diverting the gathering to substitute bearing for scrounging. Then again, the gathering is splitted into littler subgroups if the worldwide pioneer can't refresh the situation for global leader limit (GLL). Negative input is gotten from LLL and GLL for the neighborhood and worldwide pioneers to take their choices.

Weight Updating:

Initialization: Initially, the following parameters are to be initialized. Individual leader limit is initialized between [W/2, 2×W], where W is the size of swarm. General leader limit is initialized in d×W, d represents the dimensional space. Perturbation rate is initialized in the range [0.1, 0.9]. Then, candidate solutions or current position of spider monkeys (M_i) are initialized in the d^{th} dimensional space. In this approach, the weight values are represented as W_{ij} and the initial solution is given in equation (17)

$$S_{ij} = [W_{11}, W_{12}, W_{13}, ..., W_{in}] \quad (17)$$

Fitness: The best solution or the best weight is estimated by evaluating the fitness of each solution. For each solution, fitness value is calculated as follows:

$$Fitness = \max(Accuracy) \quad (18)$$

$$Accuracy = \frac{T_P + T_N}{T_P + F_P + F_N + T_N} \quad (19)$$

Best fitness value is selected initially and the best-fitness selected randomly for a general leader. If the selected local leader and global leader lack to select optimal solution, then the solutions or spider monkeys start to move for searching with the experience of individual leader and general leader. The Updation of the spider monkeys is described as follows.

Updation: This updating phase includes the following phases such as individual leader phase, general leader phase, learning phase of general leader, leaning phase of individual leader, decision phase of global leader and decision phase of individual leader. These phases of this algorithm are described as follows.

***Individual leader phase*:** In this phase, each spider monkey or solution determines its new position based on the experience of individual leader and individual group members. The new position of the spider monkey is calculated as follows,

$$M_{newi,d} = \begin{cases} M_{i,d} + r1 \times (IL_{k,d} - M_{i,d}) + r2 \times (M_{j,d} - M_{i,d}) & if\ r1 \ge PR \\ M_{i,d} & otherwise \end{cases} \quad (20)$$

Where, r_1 and $r_2$represent arbitrary number in the range [0, 1] and [-1, 1], $IL_{k,d}$ represents the position of k^{th}individual leader in the d^{th} dimension. $M_{j,d}$ presents the randomly selected spider monkey from the j^{th} group in the d^{th} dimension. *PR* represents the perturbation rate which manifests the number of perturbation.

***General leader phase*:** Individual leader phase is followed by this phase known as general leader phase. In this phase, all spider monkeys update their position with respect to the experience of individual all members and global leader. The new position of the spider monkey is calculated as follows,

$$M_{newi,d} = M_{i,d} + r_1 \times (GL_d - M_{i,d}) + r_2 \times (M_{j,d} - M_{i,d}) \quad (21)$$

Where, GL_d represents the position of general leader in the d^{th} dimension. Spider monkeys are updated their position based on the following probability value. This probability is calculated with the fitness function. The solution or spider monkey with the better probability updates its position using (22). This probability (Pr_i) value is calculated as follows:

$$\Pr_i = \frac{Fit_i}{\max - Fit} \times 0.9 + 0.1 \quad (22)$$

Where, Fit_i represents the fitness value of i^{th} spider monkey, *max-Fit* represents the maximum fitness value in the group.

***Learning phase of general leader*:** In this phase, the position of general leaders is updated and the spider monkey with the best fitness value in the population is selected as the general leader. If the position of the general leader is not updated, then the general limit count which counts the number of individual best solution is increased by 1.

***Learning phase of individual leader*:** In this phase, the position of group members is updated and the member with the best fitness value in the group is selected as the individual leader. If the position of the individual leader is not updated, then the individual limit count which counts the number of general best solution is increased by 1.

***Decision phase of individual leader*:** If individual leader count is greater than the individual leader limit, then the position of all group members are updated randomly or based on the information of individual leader and general leader. The new position of the spider monkey is calculated as follows,

$$M_{newi,d} = M_{i,d} + r_1 \times (GL_d - M_{i,d}) + r_1 \times (M_{i,d} - IL_{j,d}) \quad (23)$$

From equation (23), it is cleared that the position of the spider monkey is updated towards the position of general leader.

***Decision phase of general leader*:** In this phase, the population is divided into maximum number of small groups if the general limit count is Greater

than the general leader limit. Individual leader limit is initiated to select the individual group leader for each group in this phase. If the situation of common leader is not refreshed, at that point the general leader joints all groups together and forms a single group.

Termination: Above described phases are continued until find the optimal solution or the best weight is obtain. The selected weight is given to the PNN. Fig.3 shows the flow chart of this algorithm.

Step 7: The optimal weight value is given to the PNN and based on this weight the system will be trained. After training process, the test images are tested.

Testing process:

In the testing process, we classify given input. Initially, the testing image is given to the preprocessing and the GLCM computed features fed to the input of PNN. The trained weight value is assigned to the testing process. After the calculation, the score value (Ω) is obtained for the corresponding test image. Score value classifies images. In this work, two classes are available namely, normal or abnormal, so we fix one threshold values toclassifying the image. The threshold value is depending upon the class value only. The classification can be attained using equation (24).

$$output = \begin{cases} 0 < O^{score} < Th_1; & abnormal\ image \\ otherwise & normal\ image \end{cases} \quad (24)$$

F. Segmentation using PFCM

Let us consider the input image I which consist of stone region and normal region. These two regions are clustered from the input image. So, that the size of the cluster is 2. The proposed PFCM optimize the following objective function which is given in equation (25).

$$O_{PFCM}(U,T,V;Y) = \sum_{k=1}^{n}\sum_{i=1}^{c}(aU_{ik}^{m} + bT_{ik}^{\eta}) \times \left\| y_k - v_i \right\|_A^2 + \sum_{i=1}^{c}\gamma_i \sum_{k=1}^{n}(1-T_{ik})^{\eta} \quad (25)$$

Subject to the parameters $\sum_{i=1}^{c} U_{ik} = 1 \ \forall k$ and $0 \le U_{ik}$, $T_{ik} \le 1$. Here $a > 0$, $b > 0$, $m > 1$ and $\eta > 1$. In (1) $\gamma_i > 0$ is the user specified constant. The constant a *and* b defined the comparative significance of the fuzzy enrollment and averageness esteems in the target work. In this equation (25), U_{ik} is a membership function which is derived from the FCM. The membership function U_{ik} can be calculated as follows;

$$U_{ik} = \frac{1}{\sum_{j=1}^{c}\left(\frac{\left\| y_k - v_i \right\|}{\left\| y_k - v_j \right\|}\right)^{\frac{2}{m-1}}} \quad (26)$$

Similarly, in equation (14), typically matrix T_{ik} is similar to PCM. The typically matrix T_{ik} can be calculated as follows;

$$T_{ik} = \frac{1}{1 + \left[\frac{D^2(x_k, v_i)}{\eta_i}\right]^{1/(m-1)}} \quad (27)$$

The cluster center V_i of PFCM is can be calculated as follows;

$$v_i = \frac{\sum_{k=1}^{n}\left(au_{ik}^{m} + bt_{ik}^{\eta}\right)X_k}{\sum_{k=1}^{n}\left(au_{ik}^{m} + bt_{ik}^{\eta}\right)}, 1 \le i \le c. \quad (28)$$

The clustering process is continued on k-number of iteration. After the clustering process, the image is grouped into 2 numbers of clusters namely, normal region and stone region. Then execution of the methodology is analyzed as far as different metrics.

IV.RESULT AND DISCUSSION

This section discusses the outcome acquired from the proposed renal stone classification. We have used "512×512" estimated images which are publicly available.

A. Evaluation metrics

The framework execution is evaluated by below performance measures in terms of truepositive(T_p), truenegative T_n,falsepositive (F_p), falsenegative(F)$_n$.

Sensitivity

It is defined as extent of genuine positives that are accurately detected is the proportion of affectability.

$$Sensitivity = \frac{T_p}{T_p + F_n} \quad (29)$$

Specificity

The ratio of negatives that are properly recognized is the proportion of the particularity.

$$Specificity = \frac{T_n}{T_n + F_p} \quad (30)$$

Accuracy

We can register the proportion of accuracy from the proportions of affectability and explicitness as indicated underneath.

$$Accuracy = \frac{T_p + T_n}{T_p + F_p + F_n + T_n} \quad (31)$$

PositivePredictiveValue (PPV)

It is defined as possibility that the images identified as truly diseased.

$$PPV = \frac{TP}{TP + FP} \quad (32)$$

NegativePredictiveValue (NPV)

It is defined as that the images detected as truly do not have disease.

$$NPV = \frac{TN}{TN + FN} \quad (33)$$

False Positive Rate (FPR)

FPR is determined as the quantity of erroneous positive expectations divided by the complete number of negatives. It can likewise be determined as 1 – particularity.

$$FPR = \frac{FP}{FP + TN} \quad (34)$$

False Negative Rate (FNR)

FNR is determined as the quantity of off base negative predictions isolated by the absolute number of negatives.

$$FNR = \frac{FN}{FN + TP} \quad (35)$$

B. Experimental results

The basic idea of our methodology is disease detection in kidney ultrasound images using multiple stages. The performance is evaluated using different evaluation metrics. Here we have categorized the performance measure of both normal and abnormal kidney type. The main theme of our research work is to segment the affected portion in the abnormal kidney image. Also, we have compared our proposed work PNN-SMO with existing PNN technique. The experiment is done with kidney ultrasound dataset taken from online and their performance measures were evaluated. Some of the sample kidney ultrasounds database input images are taken for analysis is given below.

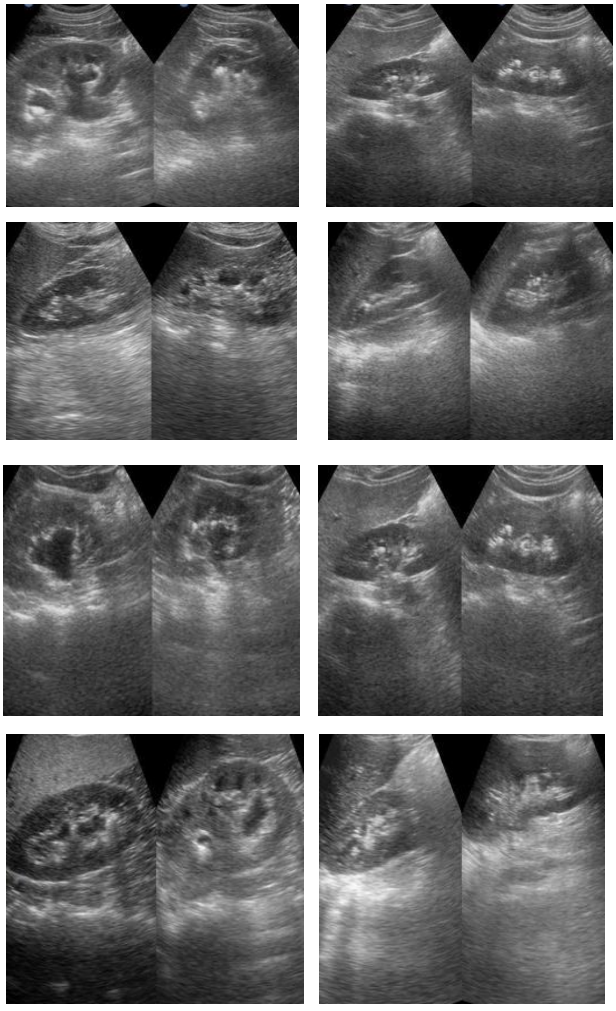

Fig.3.Set of sample kidney ultrasound images

The above sample ultrasound images are taken as input. Initially input images are fed into the preprocessing stage with the help of median filter. Then the important features were extracted by means of GLCM.

Afterwards a novel OPNN classifier is utilized to identify normal and abnormal kidney image where network structure is optimized with the help of Spider Monkey optimization algorithm. At last the affected portion is segmented by using PFCM from the obtained abnormal renal image. The input and segmented images are given in fig.4

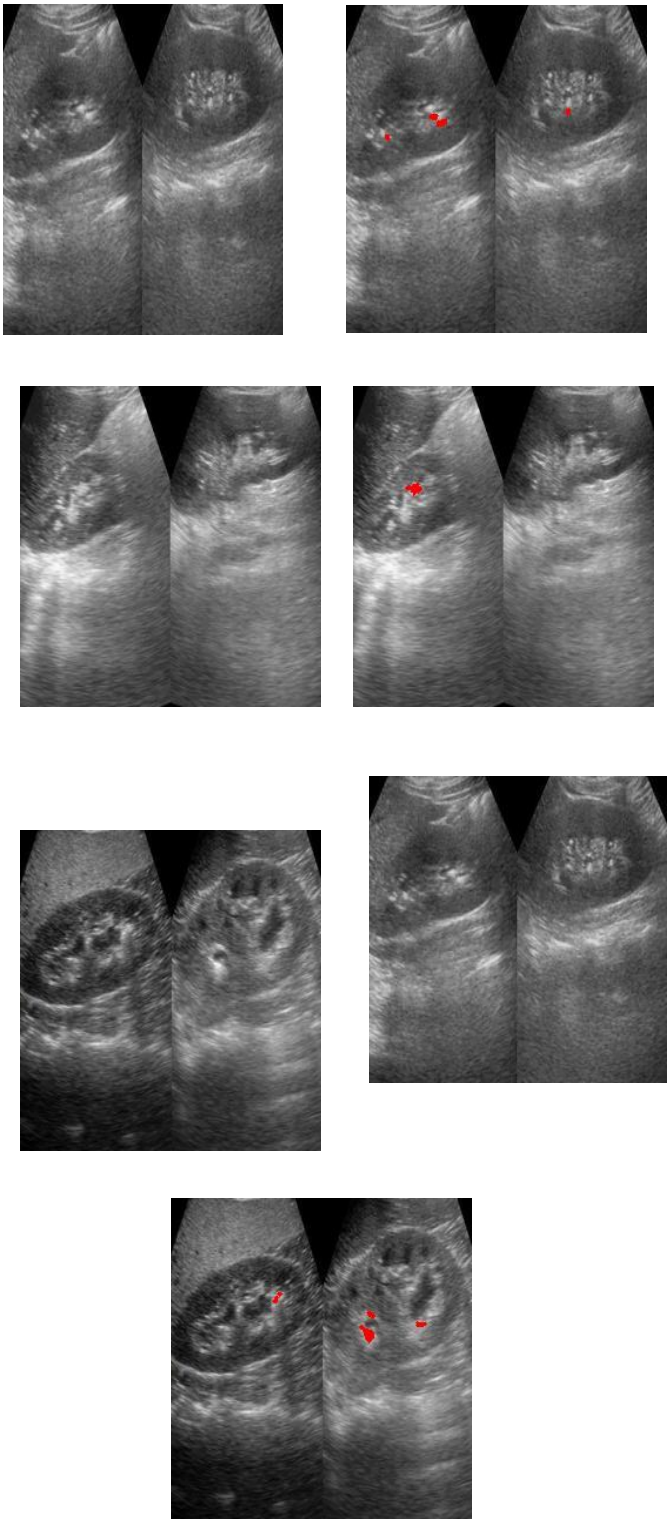

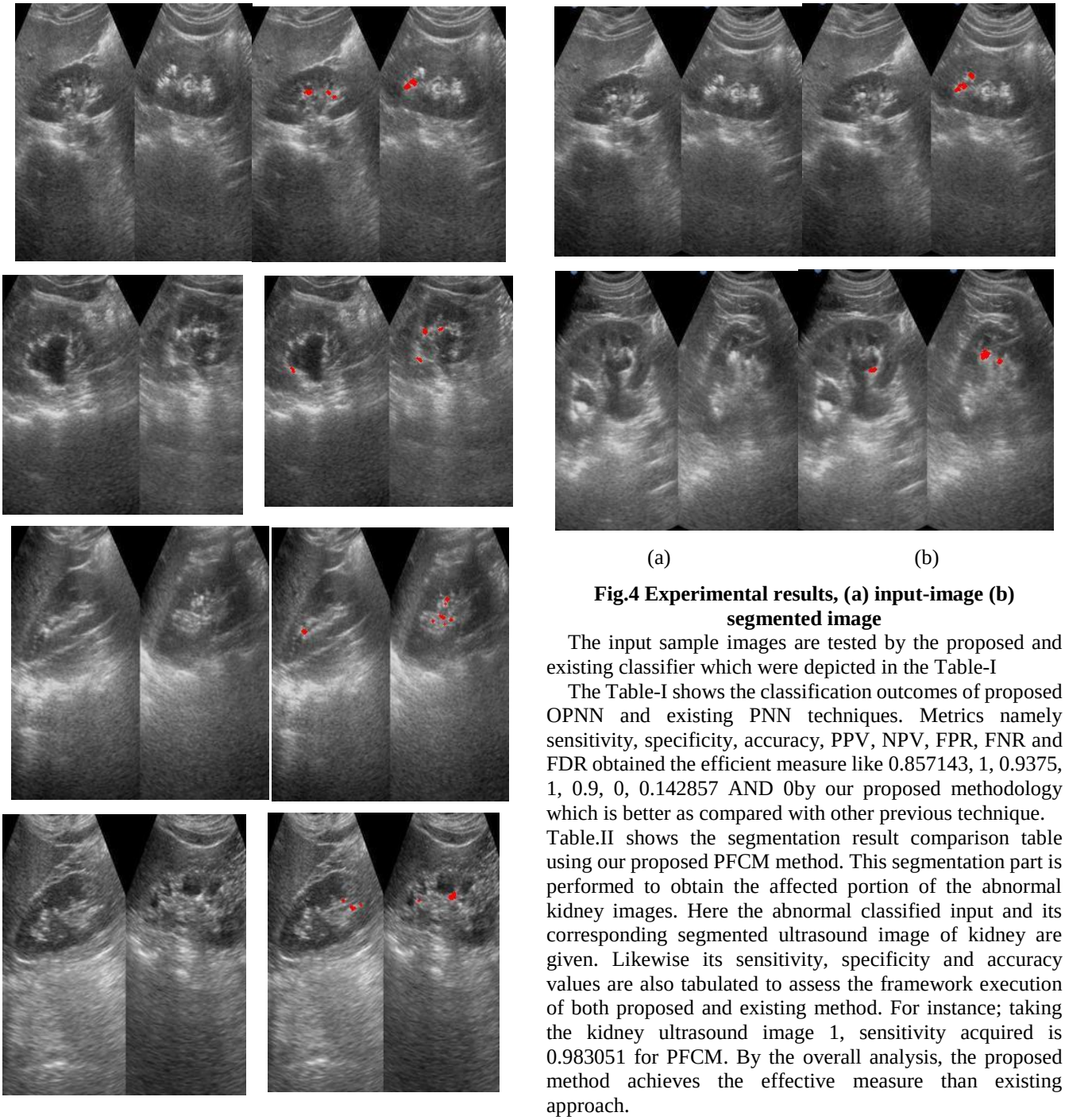

(a) (b)

Fig.4 Experimental results, (a) input-image (b) segmented image

The input sample images are tested by the proposed and existing classifier which were depicted in the Table-I

The Table-I shows the classification outcomes of proposed OPNN and existing PNN techniques. Metrics namely sensitivity, specificity, accuracy, PPV, NPV, FPR, FNR and FDR obtained the efficient measure like 0.857143, 1, 0.9375, 1, 0.9, 0, 0.142857 AND 0by our proposed methodology which is better as compared with other previous technique.

Table.II shows the segmentation result comparison table using our proposed PFCM method. This segmentation part is performed to obtain the affected portion of the abnormal kidney images. Here the abnormal classified input and its corresponding segmented ultrasound image of kidney are given. Likewise its sensitivity, specificity and accuracy values are also tabulated to assess the framework execution of both proposed and existing method. For instance; taking the kidney ultrasound image 1, sensitivity acquired is 0.983051 for PFCM. By the overall analysis, the proposed method achieves the effective measure than existing approach.

Table-I: Classification measures for proposed and existing technique

	Sensitivity	Specificity	Accuracy	PPV	NPV	FPR	FNR	FDR
OPNN	0.857143	1	0.9375	1	0.9	0	0.142857	0
PNN	0.75	0.75	0.75	0.5	0.9	0.25	0.25	0.5

Table-II: Segmented Outcome using different metrics

	Sensitivity	Specificity	Accuracy	PPV	NPV	FPR	FNR	FDR
Image 1	0.983051	1	0.999969	1	0.999969	0	0.016949	0
Image 2	0.873786	1	0.999802	1	0.999801	0	0.126214	0

Image 3	0.989247	1	0.999985	1	0.999985	0	0.010753	0
Image 4	0.951456	1	0.999924	1	0.999924	0	0.048544	0
Image 5	0.775701	1	0.999634	1	0.999633	0	0.224299	0
Image 6	0.775	1	0.999588	1	0.999587	0	0.225	0
Image 7	0.867133	1	0.99971	1	0.99971	0	0.132867	0
Image 8	0.932039	1	0.999786	1	0.999786	0	0.067961	0
Image 9	0.92	1	0.999817	1	0.999817	0	0.08	0

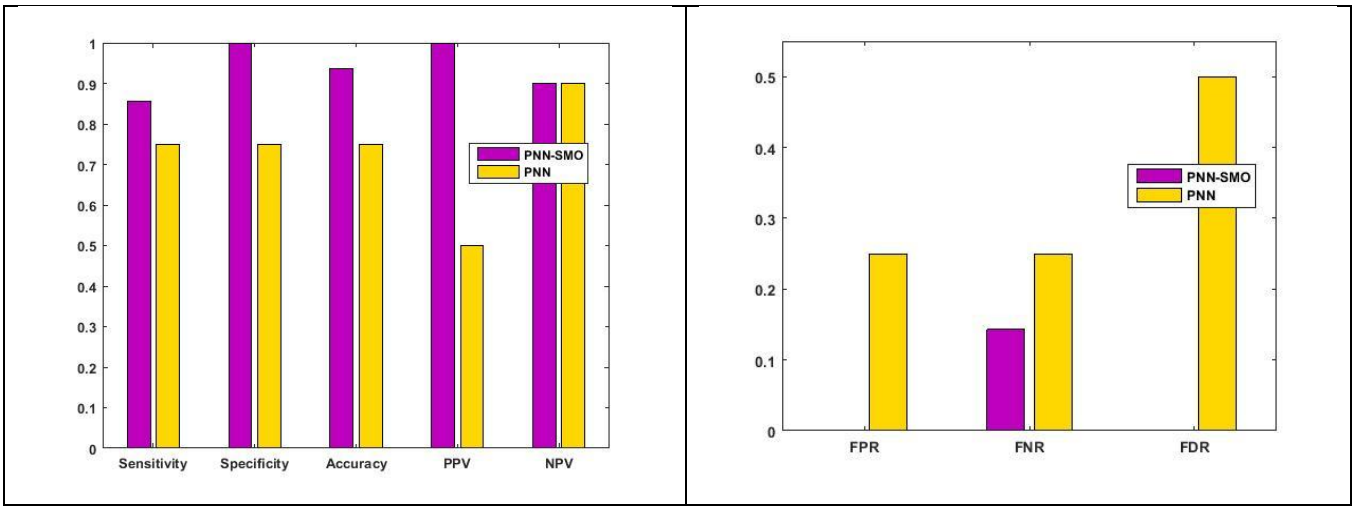

Fig .5. Comparison graph obtained by proposed and existing method for classification

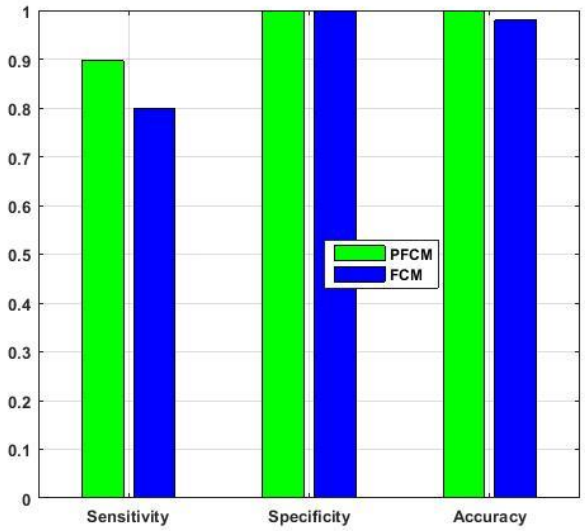

Fig. 6.Comparison plot for segmentation measure

Fig. 5 and 6 shows the comparison graph of proposed and existing methods for classification and segmentation. The bar chart is represented for sensitivity, specificity, accuracy, PPV, NPV, FPR, FNR and FDR with two color combos. All the measures attained is in maximum range expect FPR, FNR and FDR. Hence, the overall proposed system obtains minimum error rate because of the hybrid classification technique compared with the existing default PNN algorithm.

V.CONCLUSION

The fundamental point of this work is detection of the affected portion of kidney stone image. For that, the input kidney image is fed into the Pre-processing stage by utilizing the median filter; then the particular features are removed with the assistance of the GLCM approach. The extracted features are fed into a classification stage where OPNN is performed to classify normal and abnormal kidney images.

In OPNN, its network weight is optimally chosen via SMO. Finally, for the abnormal kidney image, the affected disease portion is segmented through the PFCM technique. The whole work is implemented using MATLAB software. Different evaluation metrics are taken to differentiate the proposed and existing methodology. From the overall analysis, our proposed technique achieves better results than other existing works.

REFERENCES

1. Bansal, Amar D., Jennifer Hui, and David S. Goldfarb. "Asymptomatic nephrolithiasis identified by ultrasound." Clinical Journal of the American Society of Nephrology 4, no. 3 (2009): 680-684.
2. Viswanath, Kalannagari, and RamalingamGunasundari. "Design and analysis performance of kidney stone detection from ultrasound image by level set segmentation and ANN classification." In 2014 International Conference on Advances in Computing, Communications and Informatics (ICACCI), pp. 407-414. IEEE, 2014.
3. Rahman, Tanzila, and Mohammad Shorif Uddin. "Speckle noise reduction and segmentation of kidney regions from ultrasound image." In 2013 International Conference on Informatics, Electronics and Vision (ICIEV), pp. 1-5. IEEE, 2013.
4. Tasian, Gregory E., Jose E. Pulido, Ron Keren, Andrew W. Dick, Claude M. Setodji, Jan M. Hanley, Rodger Madison, and Christopher S. Saigal. "Use of and regional variation in initial CT imaging for kidney stones." Pediatrics 134, no. 5 (2014): 909.
5. Tamilselvi, P. R., and P. Thangaraj. "Segmentation of Calculi from Ultrasound Kidney Images by Region Indictor with Contour Segmentation Method." global journal of computer science and technology (2012).
6. Akman, Tolga, Murat Binbay, Rahmi Aslan, EmrahYuruk, FarukOzgor, ErdemTekinarslan, OzgurYazici, YalcinBerberoglu, and Ahmet YaserMuslumanoglu. "Long-term outcomes of percutaneous nephrolithotomy in 177 patients with chronic kidney disease: a single center experience." The Journal of urology 187, no. 1 (2012): 173-177.
7. Masselli, G., M. Weston, and J. Spencer. "The role of imaging in the diagnosis and management of renal stone disease in pregnancy." Clinical radiology 70, no. 12 (2015): 1462-1471.
8. Cury, DídiaBismara, Alan C. Moss, and Nestor Schor. "Nephrolithiasis in patients with inflammatory bowel disease in the community." International journal of nephrology and renovascular disease 6 (2013): 139.
9. Supriyanto, Eko, NurulAfiqah Tahir, Syed MohdNooh, A. Arooj, and W. Hafizah. "Automatic ultrasound kidney's centroid detection system." In Proceedings of the 15th WSEAS international conference on Computers, pp. 160-165. World Scientific and Engineering Academy and Society (WSEAS), 2011.
10. Winkel, RikkeRass, Anna Kalhauge, and Knud-Erik Fredfeldt. "The usefulness of ultrasound colour-Doppler twinkling artefact for detecting urolithiasis compared with low dose nonenhancedcomputerizedtomography." Ultrasound in medicine & biology 38, no. 7 (2012): 1180-1187.
11. Varma, Gayathri, Nandu Nair, Abiya Salim, and YM FazilMarickar. "Investigations for recognizing urinary stone." Urological research 37, no. 6 (2009): 349.
12. Hafizah, Wan Mahani, EkoSupriyanto, and JasmyYunus. "Feature extraction of kidney ultrasound images based on intensity histogram and gray level co-occurrence matrix." In 2012 Sixth Asia Modelling Symposium, pp. 115-120. IEEE, 2012.
13. Hafizah, Wan Mahani, EkoSupriyanto, and JasmyYunus. "Feature extraction of kidney ultrasound images based on intensity histogram and gray level co-occurrence matrix." In 2012 Sixth Asia Modelling Symposium, pp. 115-120. IEEE, 2012.
14. Attia, Mariam Wagih, F. E. Z. Abou-Chadi, Hossam El-Din Moustafa, and NaghamMekky. "Classification of ultrasound kidney images using PCA and neural networks." International Journal of Advanced Computer Science and Applications 6, no. 4 (2015): 53-57.
15. Kumar, Koushal, and B. Abhishek. Artificial neural networks for diagnosis of kidney stones disease. GRIN Verlag, 2012.
16. Gupta, Abhinav, BhuvanGosain, and Sunanda Kaushal. "A comparison of two algorithms for automated stone detection in clinical B-mode ultrasound images of the abdomen." Journal of clinical monitoring and computing 24, no. 5 (2010): 341-362.
17. Bailey, M. R., V. A. Khokhlova, O. A. Sapozhnikov, S. G. Kargl, and L. A. Crum. "Physical mechanisms of the therapeutic effect of ultrasound (a review)." Acoustical Physics 49, no. 4 (2003): 369-388.

AUTHORS PROFILE

P.RAJU was born in 1982, received his B.Tech, M.E degree from Nagarjuna University and Andhra University respectively. He is a Ph.D Scholar of JNTUK,Kakinada. He is currently working as Assistant Professor, Dept. of ECE in GITAM Vishakhapatnam. Area of interest are Image Processing, Signal processing.

Dr.V.MALLESWARARAO received his B.E. degree from Andhra University and M.E. degree from Andhra University and completed his Ph.D from J.N.T.U Hyderabad. He has 23 years of teaching experience, 8 years of Research Experience and currently working in GITAM, Visakhapatnam as Professor. He produced 10 PhD's and guiding 8 PhD scholars. Area of interests are Low Power VLSI Design, Microwave, Image processing.

Dr. B. PRABHAKARARAO received his B.Tech degree, M.Tech degree from SV University, Tirupati and received the Ph.D degree from IISC, Bangalore. He has more than 28 years of teaching experience and 20 years of R & D. He is an expert in Signal Processing & Communications. He produced 15 PhD's and guiding 30 PhD scholars. He held different positions like HoD, Vice-Principal, in JNTU College of Engineering, Director (Institute of Science & Technology) and Director of Evaluation; Director of Foreign University & Alumni Relations and Rector JNT University Kakinada. He authored 17 books. He published more than 120 technical papers in National and International journals and conferences .Research areas are in Optical Communications, Microwave Communications, Coding theory, Image Processing, Satellite Communications and Signal processing.